Molecular Human Reproduction, Vol.23, No.9 pp. 607–616, 2017
Advanced Access publication on August 9, 2017 doi:10.1093/molehr/gax040

molecular human reproduction

ORIGINAL ARTICLE

Intracellular activation of ovastacin mediates pre-fertilization hardening of the zona pellucida

Hagen Körschgen[1], Michael Kuske[1], Konstantin Karmilin[1], Irene Yiallouros[1], Melanie Balbach[2], Julia Floehr[3], Dagmar Wachten[2,4], Willi Jahnen-Dechent[3], and Walter Stöcker[1,*]

[1]Institute of Molecular Physiology, Department of Biology, Johannes Gutenberg-University Mainz, 55099 Mainz, Germany [2]Max-Planck Research Group Molecular Physiology, Center of Advanced European Studies And Research (CAESAR), 53175 Bonn, Germany [3]Biointerface Laboratory, Helmholtz-Institute for Biomedical Engineering, 52074 Aachen, Germany [4]Institute of Innate Immunity, University Hospital, University of Bonn, 53175 Bonn, Germany

*Correspondence address. Tel: +49-6221-3924273; E-mail: stoecker@uni-mainz.de

Submitted on March 7, 2017; resubmitted on July 6, 2017; editorial decision on July 14, 2017; accepted on July 17, 2017

STUDY QUESTION: How and where is pro-ovastacin activated and how does active ovastacin regulate zona pellucida hardening (ZPH) and successful fertilization?

STUDY FINDING: Ovastacin is partially active before exocytosis and pre-hardens the zona pellucida (ZP) before fertilization.

WHAT IS KNOWN ALREADY: The metalloproteinase ovastacin is stored in cortical granules, it cleaves zona pellucida protein 2 (ZP2) upon fertilization and thereby destroys the ZP sperm ligand and triggers ZPH. Female mice deficient in the extracellular circulating ovastacin-inhibitor fetuin-B are infertile due to pre-mature ZPH.

STUDY DESIGN, SAMPLES/MATERIALS, METHODS: We isolated oocytes from wild-type and ovastacin-deficient (*Astl*^{null}) FVB mice before and after fertilization (*in vitro* and *in vivo*) and quantified ovastacin activity and cleavage of ZP2 by immunoblot. We assessed ZPH by measuring ZP digestion time using α-chymotrypsin and by determining ZP2 cleavage. We determined cellular distribution of ovastacin by immunofluorescence using domain-specific ovastacin antibodies. Experiments were performed at least in triplicate with a minimum of 20 oocytes. Data were pre-analyzed using Shapiro–Wilk test. In case of normal distribution, significance was determined via two-sided Student's *t*-test, whereas in case of non-normal distribution via Mann–Whitney *U*-test.

MAIN RESULTS AND THE ROLE OF CHANCE: Metaphase II (MII) oocytes contained both inactive pro-ovastacin and activated ovastacin. Immunoblot and ZP digestion assays revealed a partial cleavage of ZP2 even before fertilization in wild-type mice. Partial cleavage coincided with germinal-vesicle breakdown and MII, despite the presence of fetuin-B protein, an endogenous ovastacin inhibitor, in the follicular and oviductal fluid. Upon exocytosis, part of the C-terminal domain of ovastacin remained attached to the plasmalemma, while the N-terminal active ovastacin domain was secreted. This finding may resolve previously conflicting data showing that ovastacin acts both as an oolemmal receptor termed SAS1B (sperm acrosomal SLLP1 binding protein; SLLP, sperm lysozyme like protein) and a secreted protease mediating ZP2 cleavage.

LIMITATIONS, REASONS FOR CAUTION: For this study, only oocytes isolated from wild-type and ovastacin-deficient FVB mice were investigated. Some experiments involved oocyte activation by the Ca^{2+} ionophore A23187 to trigger ZPH.

WIDER IMPLICATIONS OF THE FINDINGS: This study provides a detailed spatial and temporal view of pre-mature cleavage of ZP2 by ovastacin, which is known to adversely affect IVF rate in mice and humans.

LARGE SCALE DATA: None.

STUDY FUNDING AND COMPETING INTEREST(S): This work was supported by the Center of Natural Sciences and Medicine and by a start-up grant of the Johannes Gutenberg University Mainz to W.S., and by a grant from Deutsche Forschungsgemeinschaft and by the START program of the Medical Faculty of RWTH Aachen University to J.F. and W.J.D. There are no competing interests to declare.

Key words: ovastacin / fetuin-B / zona pellucida / zona pellucida hardening / embryo development / hatching / IVF / polyspermy

Introduction

Upon fertilization, the mammalian oocyte exocytoses about 4000 cortical granules (CG) (Austin, 1956; Ducibella *et al.*, 1988) during the cortical reaction (Szollosi, 1967; Wessel *et al.*, 2001). This causes physico-chemical changes (Inoue and Wolf, 1975) in the extracellular matrix surrounding the egg, called the zona pellucida (ZP), which hardens and thereby gains resilience against mechanical stress (Drobnis *et al.*, 1988). Zona pellucida hardening (ZPH) occurs within minutes upon plasmogamy (Barros and Yanagimachi, 1971) and renders the egg envelope impermeable for further sperm (Smithberg, 1953; Braden *et al.*, 1954). Several possible explanations for *in vivo* ZPH in the mouse have been considered. These include, for example, the impact of zinc sparks emanating from fertilized oocytes (Que *et al.*, 2015, 2017) and the action of various enzymes released from CG such as ovoperoxidase (Schmell and Gulyas, 1980) or proteases (Gwatkin *et al.*, 1973; Wolf and Hamada, 1977; Huarte *et al.*, 1985, 1993; Zhang *et al.*, 1992). An additional cause for ZPH observed during conventional IVF was attributed to constituents of the oviductal fluid in several species (Coy and Avilés, 2010; Mondéjar *et al.*, 2013).

In the mouse *Mus musculus* the ZP is composed of three major glycoproteins, termed zona pellucida proteins ZP1, ZP2 and ZP3 (Bleil and Wassarman, 1980; Wassarman *et al.*, 2004). Upon fertilization, ZPH comes along with proteolytic conversion of ZP2 (120 kDa) into $ZP2_f$ (90 kDa + 30 kDa) (Bleil *et al.*, 1981; Moller and Wassarman, 1989) at a conserved cleavage site (^{167}LA↓DE^{170}) (Gahlay *et al.*, 2010). This cleavage impairs sperm-zona attachment and was suggested definitely to prevent polyspermy (Burkart *et al.*, 2012; Avella *et al.*, 2014). The responsible proteinase was identified as ovastacin, an astacin-family metalloproteinase encoded by the gene *Astl* (Quesada *et al.*, 2004; Burkart *et al.*, 2012). Enzymes of the astacin-family exhibit a unique specificity for peptide bonds amino-terminal of diacidic sequence motifs (Becker-Pauly *et al.*, 2011). Ovastacin is translated as an inactive zymogen (pro-ovastacin), including a secretory signal peptide (23 aa), a pro-domain (62 aa), the catalytic protease domain (200 aa) and a unique C-terminal domain (150 aa) of unknown structure and function (Quesada *et al.*, 2004; Gomis-Rüth *et al.*, 2012). The pro-domains of astacin zymogens position an invariant aspartate residue to block the catalytically essential zinc ion and, thus, removal of the pro-domain is required to gain activity (Yiallouros *et al.*, 2002; Guevara *et al.*, 2010). As shown only recently (Xiong *et al.*, 2017), the pro-domain contains in addition a signalling sequence (^{52}DKDIPAIN^{64}), which targets ovastacin to the CG *via* the regulated secretory pathway.

ZP2 cleavage by ovastacin seems to be closely linked to ZPH, since the knockout of fetuin-B, a highly specific inhibitor of ovastacin, results in precocious ZPH before fertilization and causes female infertility in mice (Dietzel *et al.*, 2013; Stöcker *et al.*, 2014). Fetuin-B was detected *in silico* (Olivier *et al.*, 2000), verified as a liver-derived plasma protein (Denecke *et al.*, 2003), and eventually identified as a potent inhibitor of ovastacin that is also present in the follicular fluid (Dietzel *et al.*, 2013). Fetuin-B-deficient oocytes undergo ZP2 into $ZP2_f$ conversion after, not before ovulation (Dietzel *et al.*, 2013). This suggests that ovastacin needs to be tightly regulated within a narrow time window to ensure successful fertilization.

Apart from triggered release of CG upon fertilization, earlier reports describe pre-mature exocytosis of CG from unfertilized oocytes during IVM, coinciding with germinal-vesicle breakdown and the extrusion of the first meiotic polar body during ovulation (Okada *et al.*, 1986; Ducibella *et al.*, 1988, 1990). Pre-mature release of ovastacin has also been suggested to be the reason for infertility of fetuin-B deficient female mice (Dietzel *et al.*, 2013). Addition of fetuin-B during IVF partially prevented ZPH and improved the fertilization rate (Schroeder *et al.*, 1990; Dietzel *et al.*, 2017). However, despite reduced ZPH in fetuin-B treated oocytes, there was no evidence of increased polyspermy (Dietzel *et al.*, 2017), contrasting the view that ZP2 cleavage is essential for preventing polyspermy (Burkart *et al.*, 2012; Avella *et al.*, 2014; Dean, 2014).

Besides its function in ZP2 cleavage, ovastacin was also described as a sperm binding partner anchored to the oolemma and termed SAS1B (sperm acrosomal SLLP1 binding protein; SLLP, sperm lysozyme like protein) (Sachdev *et al.*, 2012; Pires *et al.*, 2013, 2015). At first glance, this contradicts the ovastacin function as a secreted ZP2-cleaving proteinase. In this context the so far unknown activation process of pro-ovastacin appears to be of significant importance. Many astacins are activated extracellularly by trypsin-like serine proteases (Yiallouros *et al.*, 2002; Guevara *et al.*, 2010; Arolas *et al.*, 2012). *In vitro*, this was also shown for pro-ovastacin (Karmilin *et al.*, unpublished data). However, it is currently unknown how and where (extra or intracellularly) pro-ovastacin is activated *in vivo*. We reasoned that intracellular proteolytic activation might separate the sperm binding from the enzymatic activity of ovastacin, resolving the seemingly conflicting spatial and temporal distribution of ovastacin.

Here we report the intracellular activation of pro-ovastacin and a physiological partial cleavage of ZP2 before fertilization *in vitro* and *in vivo*, causing partial ZPH without loss of fertility. Furthermore, we show that the C-terminal domain of pro-ovastacin remains attached to the plasmalemma after active ovastacin release.

Materials and Methods

Animals—ethical approval

This study was approved by the animal welfare committee of the Federal State of Rhineland-Palatinate. Mice (strain FVB) were treated as recommended by the Federation of Laboratory Animal Science Association. Ovastacin-deficient mice ($Astl^{null}$) were a generous gift of Jurrien Dean (National Institutes of Health, Bethesda, MD, USA) (Burkart *et al.*, 2012).

Recombinant ovastacin, c-terminal domain of ovastacin and fetuin-B

Recombinant full-length murine ovastacin (UniProt Database accession: Q6HA09) and fetuin-B (UniProt: Q9QXC1) were expressed and purified as published (Dietzel *et al.*, 2013). The construct encoding the C-terminal domain of murine ovastacin (aa 286–435) with a 5′-signal-sequence of murine fetuin-B (aa 1–18), a 3′-Strep-tag-sequence and a KpnI restriction-site, was custom-cloned into the pFastBac1 vector (Thermo Fisher, Waltham, USA). Expression and purification were performed as for full-length ovastacin (Dietzel *et al.*, 2013).

Antibodies

Polyclonal rabbit anti-propeptide and anti-full-length-ovastacin antibodies were generated against the murine ovastacin-derived peptide

^{34}CSTSVPEGFTPEGSPVFQDK^{53} and full-length recombinant mouse ovastacin, respectively. Antisera were diluted 1:10 000 for immunoblot and 1:200 for immunohistochemistry. Anti-pro-catalytic-domain antibodies (anti-pro-cat) were generated by pre-absorption of anti-full-length-ovastacin antibodies with the recombinant C-terminal domain of murine ovastacin (10-times incubation over night at 4°C followed by centrifugation for 2 h at 10 000 × *g*). The supernatant of hybridomas producing the monoclonal anti-mZP2 antibody (IE-3), raised against the N-terminal region of murine ZP2 (aa114–129) (East and Dean, 1984) was diluted 1:10 for immunoblot analysis.

Oocyte and embryo collection

For superovulation 6- to 8-week-old female mice were stimulated by i.p. injection of 5IU pregnant mares serum gonadotropin (Intergonan®, Intervet GmbH, Unterschleißheim, Germany). 48 h later the ovulation was stimulated by i.p. injection of 5 IU hCG (Ovogest®, Intervet GmbH). 14 h post-hCG the mice were sacrificed and the cumulus oocyte complexes (COCs) isolated from the ampulla. For isolation of pre-ovulation (GV intact) oocytes, the mice were sacrificed at the time of the second hormone application as described (Dietzel *et al.*, 2013). For isolation of *in vivo* fertilized oocytes females were mated upon hCG application and sacrificed 12 h *post coitum*. Oocytes were denuded for immunoblot and ZP digestion by hyaluronidase (0.3 mg/ml H4272, Sigma-Aldrich, Taufkirchen, Germany) for 3–5 min in human tubular fluid (HTF)-Medium and washed three times. Incubations were performed at 37°C and 5% CO_2 in air under mineral oil (M5310, Sigma-Aldrich).

Oocyte activation and cortical granule exudate extraction

Oocytes were activated for 10 min with 2.5 µM calcium ionophore A23187 (Sigma-Aldrich) in human tubal fluid-Medium (HTF) without bovine serum albumin (BSA) (Gwatkin *et al.*, 1976; Tawia and Lopata, 1992). For ZP digestion the oocytes were washed twice in HTF without BSA and incubated for 20 min at 37°C to allow ZP2 cleavage. Cortical granule exudate was precipitated for immunoblot analysis with 10% (v/v) trichloroacetic acid and resuspended in sample-buffer.

IVF and embryo culture

Incubations were performed at 37°C and 5% CO_2 in air under mineral oil. Sperm from 12- to 16-week-old males were collected from the *cauda epididymis* and incubated for 60 min in Toyoda-Yokohama-Hosi-medium. Sperm were mixed with up to six COCs in HTF-medium to about 1×10^6 sperm/ml for 4 h. Fertilization rate was determined after 24 h. For SDS-PAGE oocytes/embryos were washed three times in HTF-medium without BSA.

ZP digestion assay

To measure the ZPH, ZP digestion using 2 mg/ml α-chymotrypsin (C4229, Sigma-Aldrich) in PBS (0.1% (w/v) PVA (polyvinylalcohol), 1 mM $CaCl_2$) was performed as reported (Gulyas and Yuan, 1985). ZP dissolution time was determined for each oocyte. Experiments were performed in triplicates with at least 20 oocytes.

SDS-PAGE and immunoblot analysis

Oocytes or 2-cell embryos were lysed in sample-buffer (187.5 mM Tris, 6% (w/v) SDS, 30% (v/v) glycerol, 1.25 M dithiothreitol, pH6.8), instantly upon preparation, applied to 12% (w/v) Tris-glycine polyacrylamide gels and separated at 180 V in running buffer (192 mM glycine, 0.05% (w/v) SDS, 25 mM Tris/HCl pH8.3). For immunoblotting proteins were transferred onto poly-vinylidene-fluoride membranes (PVDF, Immobilon-P, Merck Millipore, Darmstadt, Germany) using 40 mM glycine, 20% (v/v) ethanol, 25 mM Tris/HCl pH8.0 as cathode buffer, 20% (v/v) ethanol, 300 mM Tris/HCl pH10.4 as anode buffer at constant voltage of 20 V for 90 min. After blocking the membrane with 10% skimmed milk powder (SKM) in Tris-buffered saline (TBS) for 1 h immunodetection was performed with antibodies as indicated in TBS-T (TBS-Tween® 20) with 7.5% (w/v) SKM for 3 h at room temperature (RT). PVDF-membranes were incubated with the secondary horseradish peroxidase-coupled anti-rabbit-IgG antibody (Dianova, Berlin, Germany) or anti-rat-IgG antibody (Thermo Fisher, Waltham, USA), respectively, for 1 h at RT in TBS-T with 5% (w/v) SKM. For detection the Biorad (Hilden, Germany) Clarity ImmunoECL solution was used.

Immunofluorescence and microscopy

All steps were performed at RT in PBS containing 0.1% PVA. Cumulus-free MII oocytes and embryos were fixed in PBS with 2% (w/v) paraformaldehyde (PFA) for 1 h, saturated with 0.1 M glycine for 1 h, followed by permeabilization with PBS-T (0.4% (v/v) Tween®20) for 10 min and blocked with 10% (v/v) goat serum for 1 h. Oocytes and embryos were incubated with the primary antibody over night at 4°C in PBS-T with 0.3% (w/v) BSA. After washing three times with PBS-T, oocytes and embryos were incubated with Alexa Flour®488-conjugated goat-anti-rabbit IgG (Thermo Fisher) 1:400 for 1 h in PBS-T with 0.3% (w/v) BSA, washed three times in PBS-T and mounted in Mowiol 4–88 medium (Carl-Roth GmbH, Karlsruhe, Germany) containing 0.5 µg/ml DAPI (4.6-diamidino-2-phenyl-indole) and 25 mg/ml DABCO (1.4-diazabicyclo-[2.2.2]-octane) as specified by the manufacturer. If the samples were not permeabilized, all steps were performed in PBS. Images were obtained on a Leica DM6000B microscope with 100-fold magnification (NA 1.40) using the manufacturer's software and deconvoluted using Huygens Core Software (Scientific Volume Imaging, Hilversum, Netherlands). In all fluorescence microscopic images, brightness and contrast were adjusted equally via ImageJ (Schneider *et al.*, 2012). Brightness and contrast of immunoblots have not been adjusted to remove background signal.

Statistical analysis

Experimental data were statistically pre-analyzed, using Shapiro–Wilk test for normal distribution. In case of normal distribution, significance was determined by two-sided Student's *t*-test, in case of non-normal distribution, via Mann–Whitney *U*-test. A value of $P < 0.05$ was considered as significant.

Results

Intracellular activation of ovastacin

Unfertilized mature metaphase II (MII) oocytes contained both intact full-length pro-ovastacin and proteolytically processed ovastacin

(Fig. 1). The intact pro-ovastacin migrated as a band at 44 kDa, consisting of propeptide, catalytic domain, and C-terminal domain. We also detected a shorter form with a molecular mass of 29 kDa. The anti-propeptide antibody only detected the 44 kDa band, the anti-full-length-ovastacin antibody detected both bands (Fig. 1) indicating that the 29 kDa form lacked the propeptide (7 kDa) and part of the C-terminal domain (8 kDa). The cortical granule exudate, i.e. supernatant from oocytes after cortical reaction, revealed the same pattern, indicating that ovastacin is exocytosed as partly activated enzyme. Knockout controls proved the specificity of ovastacin antibodies (Fig. 1).

To scrutinize this result, zonae pellucidae of MII oocytes were digested using α-chymotrypsin, which is an established test for ZP robustness (Gulyas and Yuan, 1985) (Fig. 2A), resulting in prolonged digestion times in hardened ZP. Compared to unfertilized oocytes with a digestion time of 18.8 ± 7.3 min (mean ± SD, $n = 137$), oocytes activated by Ca^{2+} ionophore A23187 had a digestion time of 35.2 ± 3.2 min (mean ± SD, $n = 107$), which was almost the same as for 2-cell embryos (36.7 ± 1.2 min; mean ± SD, $n = 109$), indicating that the Ca^{2+} ionophore readily triggered the cortical reaction and, thus, ZP2 cleavage in the absence of sperm. A23187 triggered ZP2 cleavage was inhibited by fetuin-B (19.6 ± 6.2 min; mean ± SD, $n = 79$), underscoring that measured ZPH was a result of ZP2 cleavage by ovastacin (Dietzel *et al.*, 2013, 2017; Floehr *et al.*, 2017). We added serine proteinase (Pefabloc®SC) and cysteine proteinase (E64) inhibitors to the medium in order to inhibit potential extracellular activators and to ensure that the activity was due to intracellularly activated ovastacin and not to the activation of pro-ovastacin by extracellular proteases.

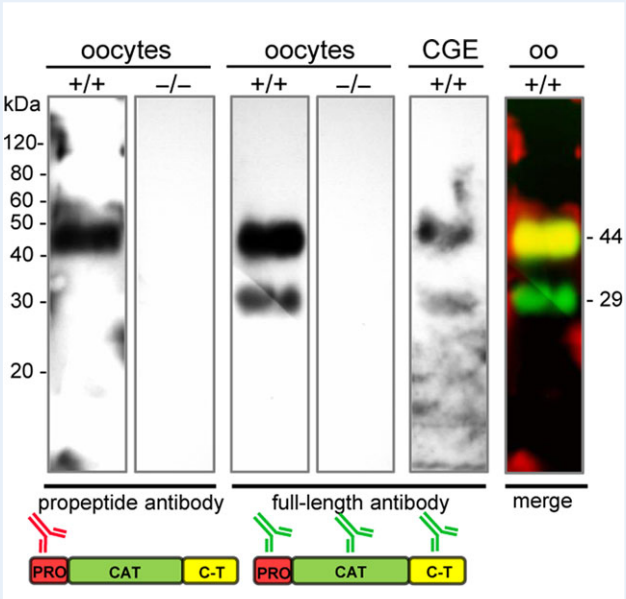

Figure 1 Immunoblot of ovastacin in oocytes lysate of 80–100 denuded wild-type oocytes (+/+), ovastacin-deficient oocytes (−/−), cortical granule exudate (CGE; on a separate gel), oo = oocytes (merge) separated via 12% SDS-PAGE, followed by immunoblotting with anti-propeptide and anti-full-length antibody. Pictogram: propeptide (red), catalytic domain (green), C-terminal domain (yellow).

However, the digestion times did not vary significantly, independent of the presence of protease inhibitors (34.9 ± 2.4 min, mean ± SD, $n = 110$ and 35.2 ± 3.2 min, mean ± SD, $n = 107$, respectively), indicating that ovastacin was not activated outside the cell. These results were confirmed by immunoblot analysis: ZP2 cleavage was increased in activated oocytes with protease inhibitors compared to untreated unfertilized oocytes (Fig. 2B).

Ovastacin partially cleaves ZP2 before fertilization, but does not affect polyspermy

The strong inhibition of ovastacin by fetuin-B prevented ZPH before fertilization and had been recognized as prerequisite for maintaining mammalian fertility (Dietzel *et al.*, 2013, 2017). However, the ZP of unfertilized wild-type MII oocytes proved to be much more resistant to proteolytic digestion (18.8 ± 7.3 min) than the ZP of ovastacin-deficient MII oocytes (1 min) (Fig. 2A), indicating partial cleavage of ZP2 by ovastacin (Fig. 2B) and partial ZPH prior to fertilization. Pre-ovulation germinal vesicle (GV) intact oocytes did not display partial cleavage of ZP2 (Fig. 2B), confirming that this cleavage was not an artefact of oocyte isolation, but occurred during natural ovulation *in vivo*. Unexpectedly, the fertilization success as such was not affected, despite increased mechanical oocyte resilience triggered by this pre-fertilization cleavage (Fig. 2C). *In vivo*, there was no decrease in the fertilization rate of ovastacin-deficient oocytes compared to the wild-type (Fig. 2C) and *in vitro*, ovastacin-deficient oocytes had even a higher fertilization rate ($P = 0.043$; Fig. 2C) than wild-types. Therefore, analyzing fertilization itself is not sufficient to explain the significant decrease in fecundity of ovastacin-deficient mice ($P < 0.0001$; Fig. 2D).

Localization of ovastacin upon fertilization

The localization and release of ovastacin was assessed by immunofluorescence microscopy (Fig. 3). The signal of the propeptide disappeared upon fertilization, indicating pro-ovastacin to ovastacin conversion. However, the catalytic and C-terminal domain were detectable—albeit in reduced quantities—up to the 2-cell embryo stage (Fig. 3). Notably, non-permeabilized MII oocytes revealed the same staining pattern (Fig. 4C2) as permeabilized MII oocytes (Fig. 3), suggesting that residual ovastacin seemed to be located at the extracellular face of the plasmalemma. To clarify, which part of ovastacin accounts for this residual signal, we sequentially pre-absorbed the anti-full-length-ovastacin antibodies by adding the purified recombinant C-terminal domain of murine ovastacin (Fig. 4A). This pre-absorbed anti-pro-cat antibody detected both isoforms of the recombinant pro-ovastacin (54 and 46 kDa), but not the C-terminal domain (Fig. 4B). Images of unfertilized permeabilized MII oocytes obtained with either anti-pro-ovastacin or anti-pro-cat antibody did not exhibit significant differences (Fig. 4C1), ensuring the comparability of the antibodies. However, in the embryos, we observed much lower signal intensity ($P = 0.019$) with the anti-pro-cat antibody (Fig. 4C3), indicating that only the C-terminal domain remained at the outer surface of the plasmalemma. The C-terminal domain was also detected in unfertilized MII oocytes ($P = 0.00038$) in the area of the oolemma surrounding the first polar body (Fig 4C2). These results suggested that the C-terminal domain of ovastacin accumulated at the outer surface of the plasmalemma, regardless of the time of ovastacin release. We also tested the antibody raised against the C-terminal domain of ovastacin

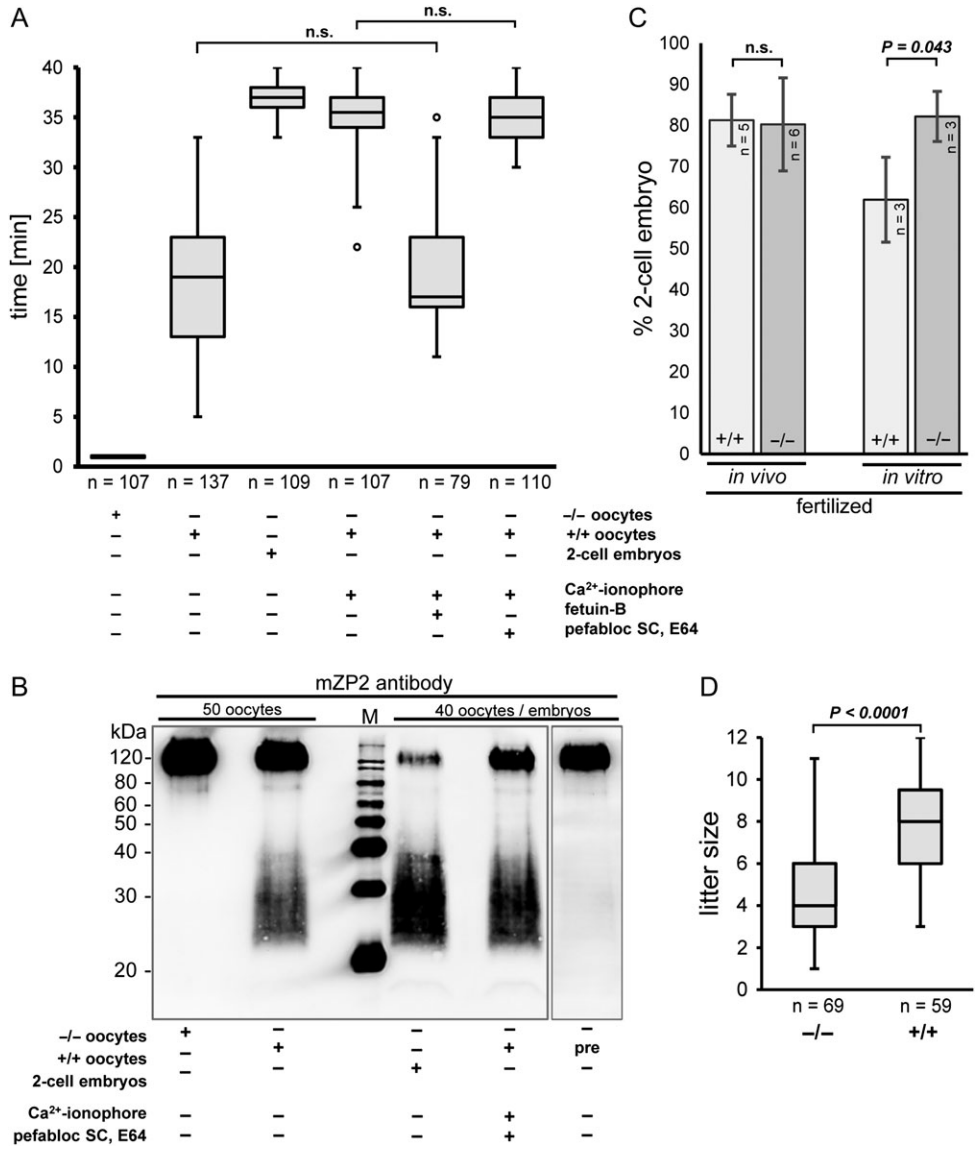

Figure 2 Effect of ovastacin on zona pellucida hardening, ZP2 cleavage and fertilization rate (**A**) α-chymotrypsin zona pellucida (ZP) digestion of wild-type oocytes (+/+), ovastacin-deficient (−/−) oocytes and 2-cell embryos. ∘ = outlier; *n*: total oocytes. Addition of fetuin-B (2.5 μM), pefabloc (250 μM) and E64 (50 μM) was simultaneous to the activation of oocytes by Ca^{2+} ionophore (2.5 μM). All experiments are statistically significant ($P < 0.01$) via Mann–Whitney *U*-test, except indicated as n.s. (non-significant). (**B**) Lysate of denuded (+/+), (−/−), pre-ovulation (pre) oocytes and embryos separated via 12% SDS-PAGE, followed by immunoblotting with anti-mZP2 antibody. (**C**) Fertilization rate (2-cell-embryos) after *in vivo* fertilisation or IVF, respectively; *n* = number of experiments (each with at least 25 oocytes); error bars: standard deviation; statistical analysed via *t*-test. (**D**) Size of litters of wild-type (+/+) and ovastacin-deficient (−/−) mice; *n* = number of analysed litters mated over a period of 24 months; statistically analysed via *t*-test.

(Burkart *et al.*, 2012) resulting in almost identical residual signal intensity at the plasmalemma of wild-type embryos (see supplemental Fig. 1) as obtained with the anti-full-length antibody.

Discussion

Several lines of evidence indicate the importance of limited proteolysis for ZPH in mammalian oocytes after fertilization. As a measure of ZPH, proteolytic *in vitro* ZP digestion has been established to distinguish freshly ovulated, unfertilized 'soft' eggs from robust 2-cell embryos (Smithberg, 1953; Braden *et al.*, 1954). A key event during zona conversion is the cleavage of ZP2 by the cortical granule (CG) metalloproteinase ovastacin at a strictly conserved site (Burkart *et al.*, 2012). ZPH is absent in ovastacin-deficient mice (Fig. 2A) and can be prevented during IVF upon addition of the highly selective physiological ovastacin-inhibitor fetuin-B (Dietzel *et al.*, 2013). Hence, the

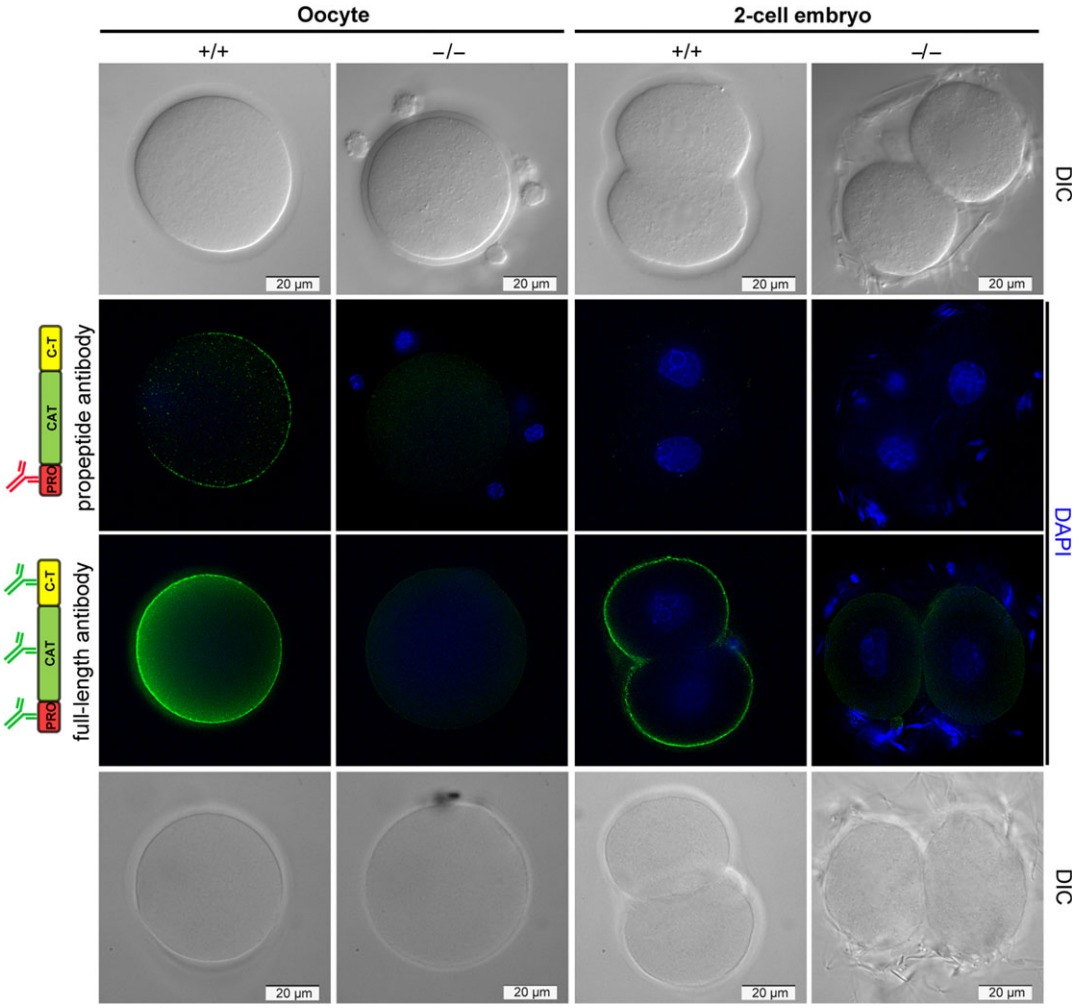

Figure 3 Ovastacin in permeabilized oocytes and embryos Light microscopic images of wild-type (+/+), ovastacin-deficient (−/−) unfertilized oocytes and in vitro fertilized 2-cell embryos. Detected with anti-propeptide and anti-full-length-ovastacin antibody and secondary antibody (Alexa Flour®488-conjugated goat-anti-rabbit IgG) (green), DAPI (blue); differential interference contrast (DIC). Magnification: 100×. Pictogram: propeptide (red), catalytic domain (green), C-terminal domain (yellow).

immunodetection of the distinct ovastacin-caused $ZP2_f$ fragments is likewise due to the action of ovastacin and consequently indicative for ZPH (Fig. 2B).

In addition to ovastacin, several serine proteinases including tissue plasminogen activator (tPA) are released from CG upon fertilization and, thus, the tPA/plasmin network is most likely involved in ZP conversion (Wolf and Hamada, 1977; Huarte *et al.*, 1985; Zhang *et al.*, 1992; Coy *et al.*, 2012; Peng *et al.*, 2012). Indeed, the pro-ovastacin zymogen is readily converted into active ovastacin by trypsin-like serine proteinases *in vitro*, e.g. by plasmin or—even more efficient—by a combination of plasminogen and tPA (Karmilin *et al.*, unpublished data). Mouse CG contain tPA (Huarte *et al.*, 1985), but are devoid of plasminogen, which is present in the follicular fluid and oviductal fluid (Canipari *et al.*, 1987; Coy *et al.*, 2012).

This setup would consistently explain the extracellular activation of ovastacin by tPA-activated plasmin after fertilization. However, here we present evidence for partial intracellular activation of ovastacin before fertilization and the cortical reaction. This was unexpected, since most astacin-proteinase zymogens are activated extracellularly (Gomis-Rüth *et al.*, 2012). Other examples for intracellular activation are the BMP1/tolloid-astacins, which process collagens, proteoglycans, growth factors and growth factor antagonists (Gomis-Rüth *et al.*, 2012). The BMP1/tolloid-enzymes are activated by furin-like pro-protein convertases in the trans-Golgi-network (Leighton and Kadler, 2003). A similar activation process occurring on the regulated secretory pathway could also be involved in the intracellular activation of pro-ovastacin. It would explain observations like precocious ZPH during IVF, even in the absence of potential activators, such as trypsin-like serine proteinases. It remains to be elucidated, whether the intracellular activation of ovastacin in mice, which does not rely on extracellular activators in the oviductal fluid, is occurring also in other species. The limited influence of oviductal fluid (Mondéjar *et al.*, 2013) on ZPH in humans and mice appears in agreement with intracellular activation. It also remains to be clarified, whether the hardening effect of the

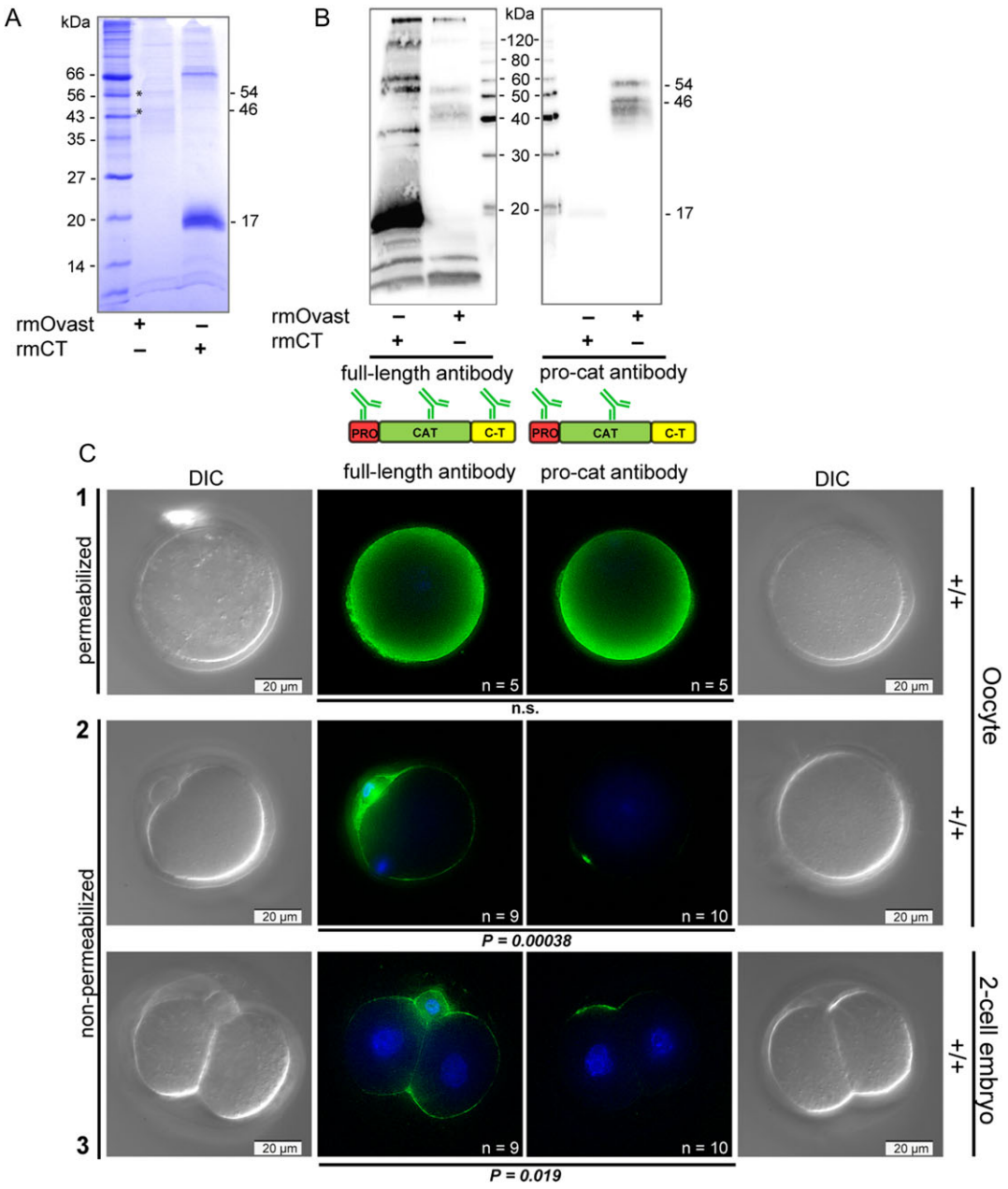

Figure 4 Antibody pre-absorption and remaining ovastacin after fertilization (**A**) 14% SDS-PAGE (Coomassie-stained) of recombinant murine full-length ovastacin (rmOvast) and recombinant murine C-terminal ovastacin domain (rmCT), rmOvast specific bands are marked by asterisks. (**B**) Immunoblot of (A) detected by anti-full-length and pre-absorbed anti-pro-cat antibody. (**C**) Light microscope pictures of unfertilized oocytes and in vivo fertilized 2-cell embryos of wild-type (+/+) mice stained with the anti-full-length and anti-pro-cat antibody and secondary antibody (Alexa Flour®488-conjugated goat-anti-rabbit IgG (green), DAPI (blue); DIC. Magnification: 100× (NA. 1.4). (**1**) Unfertilized permeabilized oocytes. (**2**) Unfertilized oocytes, non-permeabilized (**3**) *in vivo* fertilized embryos, non-permeabilized. *n* = sample size. Statistical analysis of the fluorescence intensity (integrated density of ROI (grey)) via Mann–Whitney *U*-test. Pictogram: propeptide (red), catalytic domain (green), C-terminal domain (yellow).

oviductal fluid reported for other species is due to extracellular activation of ovastacin or caused by an entirely different, unknown mechanism, which increases the chance of monospermic fertilization.

The partial intracellular activation of ovastacin also might provide a better understanding of the surprising fact that the ZP of freshly ovulated, unfertilized wild-type oocytes turned out to be 'harder' than the ZP of ovastacin-deficient oocytes. This was supported by immunodetection of $ZP2_f$ in wild-type oocytes, whereas *Astl*$^{-/-}$ oocytes and pre-ovulation wild-type oocytes did not show ZP2 cleavage. The heterogeneously sized cleavage products observed in the immunoblot (Fig. 2C) are presumably due to additional diacidic ovastacin cleavage sites in the vicinity of the crucial LA*DE-site; this has been already discussed

(Burkart et al., 2012). Hence, we present evidence for *in vivo* pre-fertilization cleavage of ZP2 in mice. Importantly, this partial zona pre-hardening does not prevent fertilization by sperm, because the strong inhibition of ovastacin by fetuin-B prevents complete ZPH, thereby maintaining fertility (Dietzel et al., 2017).

A slight pre-fertilization cleavage of ZP2 during IVM, even in the presence of serum (and, hence, in the presence of then unknown fetuin-B) had been reported earlier (Ducibella et al., 1990). Although, a more recent publication (Deng et al., 2003) favoured the view that pre-mature CG exocytosis might be only a minor side effect, occurring concomitantly with the establishment of the cortical granule free domain (CGFD) close to the first polar body. Deng et al. (2003) used the membrane permeating Ca^{2+}-chelator BAPTA-AM to ensure the absence of CG exocytosis during CGFD establishment, which was proven by the absence of proteolytic ZP2 to $ZP2_f$ conversion. However, ovastacin, being a zinc-metalloproteinase (which was not known at that time), would be most effectively inhibited by BAPTA-AM (Rosenfeldt et al., 2005), which binds Zn^{2+} much better than Ca^{2+} (Stork and Li, 2006).

The absence of ZP2 cleavage had been suggested to be associated to polyspermy (Burkart et al., 2012; Avella et al., 2014; Dean, 2014). However, contrary to this view, an inactivating mutation of the cleavage site in ZP2 did not cause polyspermy (Gahlay et al., 2010) and even the complete absence of the ZP did not reduce fertilization rate *in vitro* (Xiong et al., 2017). Inhibiting ZPH with fetuin-B *in vitro* likewise did not result in polyspermy (Dietzel et al., 2017) and oocytes from ovastacin/fetuin-B double deficient mice bound high numbers of sperm *in vitro*, but showed no signs of polyspermy (Floehr et al., 2017). Our results confirm these observations *in vivo*, demonstrating that ovastacin-deficient zygotes develop normally until the 2-cell stage. Since polyspermy already compromises the development of 2-cell embryos (Clarke and Masui, 1986), the normal development of 2-cell embryos in the absence of ovastacin, and consequently of ZP2 cleavage, does not seem to significantly affect the rate of polyspermy. It seems undisputable that ZP2 cleavage triggers ZPH and thereby provides a definitive block against polyspermy (Dean, 2014). However, before this definitive block is installed, the first sperm has fused with the oolemma and triggered a cascade of events excluding further sperm from penetrating the egg's membrane. Recent literature strongly suggests that the sperm protein IZUMO1 and the interacting oocyte protein JUNO (Bianchi et al., 2014), whose structures were solved recently (Aydin et al., 2016; Han et al., 2016; Ohto et al., 2016), prevent polyspermy by regulating sperm-oolemma interactions (Wolf and Soper, 1978; Sato, 1979).

This leaves the question, why ovastacin-deficient mice have only half-sized litters compared to wild-types (Fig. 2D). Possibly, subfertility of ovastacin-deficient mice might rather be caused by resorption of early embryos devoid of a mechanically robust ZP, as observed in embryos carrying mutations affecting the integrity of the ZP (Liu et al., 1996; Rankin et al., 1996, 1999, 2001). The slightly reduced fertilization rate of *in vitro* fertilized wild-type oocytes could be due to the absence of fetuin-B and caused by ovastacin released from bystander zygotes. Likewise, the significantly higher serum concentration of fetuin-B in mice compared to humans (Denecke et al., 2003) might be an evolutionary adaptation, which—due to higher fecundity in rodents—could protect unfertilized oocytes from ZP2 cleavage caused by ovastacin released from already fertilized eggs (Moller and Wassarman, 1989).

In conclusion, we observe *in vivo* two rounds of ZP2 cleavage, with the first round occurring immediately before or concomitantly with ovulation and the second round being the consequence of the massive burst of ovastacin activity in the cortical reaction. The physiological function of this stepwise hardening remains unclear. However, since ZP-free oocytes have higher IVF rates (Xiong et al., 2017), the pre-hardening potentially favours the fittest sperm, effectively introducing a quality control checkpoint for spermatozoa.

Beyond that, we revealed an accumulation of the C-terminal domain of ovastacin at the surface of the plasmalemma, regardless of the time of ovastacin release. These results were confirmed with the anti-C-terminal antibody (Burkart et al., 2012) (see supplemental Fig. 1). In a recent study by (Xiong et al., 2017) using ovastacin C-terminally tagged with mCherry, a remaining C-terminal domain was not observed. This might be due to an impaired binding of the processed C-terminal domain (unprocessed 15 kDa) to the plasmalemma caused by the tag (28.8 kDa).

A membrane-bound protease domain, as proposed based on *in silico* analysis (Pires et al., 2013), would render ZP2 cleavage by ovastacin unlikely. This molecular model suggested that the central part of the catalytic proteinase domain of ovastacin might be involved in anchoring the protein within the oolemma (Pires et al., 2013). However, this would disrupt the active site structure and the substrate binding cleft, which is conserved in astacin proteases (e.g. Bode et al., 1992; Guevara et al., 2010; Arolas et al., 2012). A membrane-bound C-terminal domain would reconcile these seemingly conflicting data. The C-terminal domain might act as binding partner, whereas the released protease domain could process ZP2. The existence of the 29 kDa catalytically active ovastacin and the residual part of ovastacin C-terminal domain remaining on the embryo plasmalemma would fully support this notion.

Supplementary data

Supplementary data are available at *Molecular Human Reproduction* online.

Acknowledgements

We thank Jurrien Dean (National Institutes of Health, Bethesda, MD, USA) for providing the ovastacin-deficient mouse line ($Astl^{null}$) and anti-ovastacin-antibody.

Authors' roles

Participation in study design: H.W., M.K., K.K., J.F., I.Y., W.S. Execution of experiments: H.W., M.K., M.B. Data analysis: H.W., M.K., K.K., I.Y., W.S. Contribution of reagents/materials/analysis tools: J.F., M.B., D.W., I.Y., W.J.D., W.S. Writing of the manuscript: H.W., D.W., W.J.D., W.S.

Funding

This work was supported by the Centre of Natural Sciences and Medicine and by a start-up grant of the Johannes Gutenberg University Mainz to WS, and by a grant from Deutsche Forschungsgemeinschaft and by the START program of the Medical Faculty of RWTH Aachen University to JF and WJD.

Conflicts of interest

None declared.

References

Arolas JL, Broder C, Jefferson T, Guevara T, Sterchi EE, Bode W, Stöcker W, Becker-Pauly C, Gomis-Rüth FX. Structural basis for the sheddase function of human meprin β metalloproteinase at the plasma membrane. *Proc Natl Acad Sci USA* 2012;**109**:16131–16136.

Austin CR. Cortical granules in hamster eggs. *Exp Cell Res* 1956;**10**:533–540.

Avella MA, Baibakov B, Dean J. A single domain of the ZP2 zona pellucida protein mediates gamete recognition in mice and humans. *J Cell Biol* 2014;**205**:801–809.

Aydin H, Sultana A, Li S, Thavalingam A, Lee JE. Molecular architecture of the human sperm IZUMO1 and egg JUNO fertilization complex. *Nature* 2016;**534**:562–565.

Barros C, Yanagimachi R. Induction of zona reaction in golden hamster eggs by cortical granule material. *Nature* 1971;**233**:268–269.

Becker-Pauly C, Barré O, Schilling O, Auf Dem Keller U, Ohler A, Broder C, Schütte A, Kappelhoff R, Stöcker W, Overall CM. Proteomic analyses reveal an acidic prime side specificity for the astacin metalloprotease family reflected by physiological substrates. *Mol Cell Proteomics* 2011;**10**: M111.009233.

Bianchi E, Doe B, Goulding D, Wright GJ. Juno is the egg Izumo receptor and is essential for mammalian fertilization. *Nature* 2014;**508**:483–487.

Bleil JD, Beall CF, Wassarman PM. Mammalian sperm-egg interaction: fertilization of mouse eggs triggers modification of the major zona pellucida glycoprotein, ZP2. *Dev Biol* 1981;**86**:189–197.

Bleil JD, Wassarman PM. Structure and function of the zona pellucida: identification and characterization of the proteins of the mouse oocyte's zona pellucida. *Dev Biol* 1980;**76**:185–202.

Bode W, Gomis-Rüth FX, Huber R, Zwilling R, Stöcker W. Structure of astacin and implications for activation of astacins and zinc-ligation of collagenases. *Nature* 1992;**358**:164–167.

Braden AW, Austin CR, David HA. The reaction of zona pellucida to sperm penetration. *Aust J Biol Sci* 1954;**7**:391–409.

Burkart AD, Xiong B, Baibakov B, Jimenez-Movilla M, Dean J. Ovastacin, a cortical granule protease, cleaves ZP2 in the zona pellucida to prevent polyspermy. *J Cell Biol* 2012;**197**:37–44.

Canipari R, O'Connell ML, Meyer G, Strickland S. Mouse ovarian granulosa cells produce urokinase-type plasminogen activator, whereas the corresponding rat cells produce tissue-type plasminogen activator. *J Cell Biol* 1987;**105**:977–981.

Clarke HJ, Masui Y. Transformation of sperm nuclei to metaphase chromosomes in the cytoplasm of maturing oocytes of the mouse. *J Cell Biol* 1986;**102**:1039–1046.

Coy P, Avilés M. What controls polyspermy in mammals, the oviduct or the oocyte? *Biol Rev Camb Philos Soc* 2010;**85**:593–605.

Coy P, Jimenez-Movilla M, García-Vázquez FA, Mondéjar I, Grullón L, Romar R. Oocytes use the plasminogen-plasmin system to remove supernumerary spermatozoa. *Hum Reprod* 2012;**27**:1985–1993.

Dean J. A ZP2 cleavage model of gamete recognition and the postfertilization block to polyspermy. In: Sawada H, Inoue N, Iwano M (eds). *Sexual Reproduction in Animals and Plants*. Heidelberg: Springer, 2014:401–408. DOI10.1007/978-4-431-54589-7_33.

Denecke B, Gräber S, Schäfer C, Heiss A, Wöltje M, Jahnen-Dechent W. Tissue distribution and activity testing suggest a similar but not identical function of fetuin-B and fetuin-A. *Biochem J* 2003;**376**:135–145.

Deng M, Kishikawa H, Yanagimachi R, Kopf GS, Schultz RM, Williams CJ. Chromatin-mediated cortical granule redistribution is responsible for the formation of the cortical granule-free domain in mouse eggs. *Dev Biol* 2003;**257**:166–176.

Dietzel E, Floehr J, van de Leur E, Weiskirchen R, Jahnen-Dechent W. Recombinant fetuin-B protein maintains high fertilization rate in cumulus cell-free mouse oocytes. *Mol Hum Reprod* 2017;**23**:25–33.

Dietzel E, Wessling J, Floehr J, Schäfer C, Ensslen S, Denecke B, Rösing B, Neulen J, Veitinger T, Spehr M *et al*. Fetuin-B, a liver-derived plasma protein is essential for fertilization. *Dev Cell* 2013;**25**:106–112.

Drobnis EZ, Andrew JB, Katz DF. Biophysical properties of the zona pellucida measured by capillary suction: is zona hardening a mechanical phenomenon? *J Exp Zool* 1988;**245**:206–219.

Ducibella T, Anderson E, Albertini DF, Aalberg J, Rangarajan S. Quantitative studies of changes in cortical granule number and distribution in the mouse oocyte during meiotic maturation. *Dev Biol* 1988;**130**: 184–197.

Ducibella T, Kurasawa S, Rangarajan S, Kopf GS, Schultz RM. Precocious loss of cortical granules during mouse oocyte meiotic maturation and correlation with an egg-induced modification of the zona pellucida. *Dev Biol* 1990;**137**:46–55.

East IJ, Dean J. Monoclonal antibodies as probes of the distribution of ZP-2, the major sulfated glycoprotein of the murine zona pellucida. *J Cell Biol* 1984;**98**:795–800.

Floehr J, Dietzel E, Schmitz C, Chappell A, Jahnen-Dechent W. Down-regulation of the liver-derived plasma protein fetuin-B mediates reversible female infertility. *Mol Hum Reprod* 2017;**23**:34–44.

Gahlay G, Gauthier L, Baibakov B, Epifano O, Dean J. Gamete recognition in mice depends on the cleavage status of an egg's zona pellucida protein. *Science* 2010;**329**:216–219.

Gomis-Rüth FX, Trillo-Muyo S, Stöcker W. Functional and structural insights into astacin metallopeptidases. *Biol Chem* 2012;**393**:1027–1041.

Guevara T, Yiallouros I, Kappelhoff R, Bissdorf S, Stöcker W, Gomis-Rüth FX. Proenzyme structure and activation of astacin metallopeptidase. *J Biol Chem* 2010;**285**:13958–13965.

Gulyas BJ, Yuan LC. Cortical reaction and zona hardening in mouse oocytes following exposure to ethanol. *J Exp Zool* 1985;**233**:269–276.

Gwatkin RB, Rasmusson GH, Williams DT. Induction of the cortical reaction in hamster eggs by membrane-active agents. *J Reprod Fertil* 1976;**47**: 299–303.

Gwatkin RB, Williams DT, Hartmann JF, Kniazuk M. The zona reaction of hamster and mouse eggs: production in vitro by a trypsin-like protease from cortical granules. *J Reprod Fertil* 1973;**32**:259–265.

Han L, Nishimura K, Sadat Al Hosseini H, Bianchi E, Wright GJ, Jovine L. Divergent evolution of vitamin B9 binding underlies Juno-mediated adhesion of mammalian gametes. *Curr Biol* 2016;**26**:R100–R101.

Huarte J, Belin D, Vassalli JD. Plasminogen activator in mouse and rat oocytes: induction during meiotic maturation. *Cell* 1985;**43**:551–558.

Huarte J, Vassalli JD, Belin D, Sakkas D. Involvement of the plasminogen activator/plasmin proteolytic cascade in fertilization. *Dev Biol* 1993;**157**: 539–546.

Inoue M, Wolf DP. Fertilization-associated changes in the murine zona pellucida: a time sequence study. *Biol Reprod* 1975;**13**:546–551.

Leighton M, Kadler KE. Paired basic/Furin-like proprotein convertase cleavage of Pro-BMP-1 in the trans-Golgi network. *J Biol Chem* 2003; **278**:18478–18484.

Liu C, Litscher ES, Mortillo S, Sakai Y, Kinloch RA, Stewart CL, Wassarman PM. Targeted disruption of the mZP3 gene results in production of eggs lacking a zona pellucida and infertility in female mice. *Proc Natl Acad Sci USA* 1996;**93**:5431–5436.

Moller CC, Wassarman PM. Characterization of a proteinase that cleaves zona pellucida glycoprotein ZP2 following activation of mouse eggs. *Dev Biol* 1989;**132**:103–112.

Mondéjar I, Martínez-Martínez I, Avilés M, Coy P. Identification of potential oviductal factors responsible for zona pellucida hardening and monospermy during fertilization in mammals. *Biol Reprod* 2013;**89**:67.

Ohto U, Ishida H, Krayukhina E, Uchiyama S, Inoue N, Shimizu T. Structure of IZUMO1-JUNO reveals sperm-oocyte recognition during mammalian fertilization. *Nature* 2016;**534**:566–569.

Okada A, Yanagimachi R, Yanagimachi H. Development of a cortical granule-free area of cortex and the perivitelline space in the hamster oocyte during maturation and following ovulation. *J Submicrosc Cytol* 1986;**18**:233–247.

Olivier E, Soury E, Ruminy P, Husson A, Parmentier F, Daveau M, Salier JP. Fetuin-B, a second member of the fetuin family in mammals. *Biochem J* 2000;**350**:589–597.

Peng Q, Yang H, Xue S, Shi L, Yu Q, Kuang Y. Secretome profile of mouse oocytes after activation using mass spectrum. *J Assist Reprod Genet* 2012;**29**:765–771.

Pires ES, D'Souza RS, Needham MA, Herr AK, Jazaeri AA, Li H, Stoler MH, Anderson-Knapp KL, Thomas T, Mandal A *et al*. Membrane associated cancer-oocyte neoantigen SAS1B/ovastacin is a candidate immunotherapeutic target for uterine tumors. *Oncotarget* 2015;**6**:30194–30211.

Pires ES, Hlavin C, Macnamara E, Ishola-Gbenla K, Doerwaldt C, Chamberlain C, Klotz K, Herr AK, Khole A, Chertihin O *et al*. SAS1B protein [ovastacin] shows temporal and spatial restriction to oocytes in several eutherian orders and initiates translation at the primary to secondary follicle transition. *Dev Dyn* 2013;**242**:1405–1426.

Que EL, Bleher R, Duncan FE, Kong BY, Gleber SC, Vogt S, Chen S, Garwin SA, Bayer AR, Dravid VP *et al*. Quantitative mapping of zinc fluxes in the mammalian egg reveals the origin of fertilization-induced zinc sparks. *Nat Chem* 2015;**7**:130–139.

Que EL, Duncan FE, Bayer AR, Philips SJ, Roth EW, Bleher R, Gleber SC, Vogt S, Woodruff TK, O'Halloran TV. Zinc sparks induce physiochemical changes in the egg zona pellucida that prevent polyspermy. *Integr Biol (Camb)* 2017;**9**:135–144.

Quesada V, Sánchez LM, Alvarez J, López-Otín C. Identification and characterization of human and mouse ovastacin: a novel metalloproteinase similar to hatching enzymes from arthropods, birds, amphibians, and fish. *J Biol Chem* 2004;**279**:26627–26634.

Rankin T, Familari M, Lee E, Ginsberg A, Dwyer N, Blanchette-Mackie J, Drago J, Westphal H, Dean J. Mice homozygous for an insertional mutation in the Zp3 gene lack a zona pellucida and are infertile Mice homozygous for an insertional mutation in the Zp3 gene lack a zona pellucida and are infertile. *Development* 1996;**122**:2903–2910.

Rankin T, Talbot P, Lee E, Dean J. Abnormal zonae pellucidae in mice lacking ZP1 result in early embryonic loss. *Development* 1999;**126**:3847–3855.

Rankin TL, O'Brien M, Lee E, Wigglesworth K, Eppig J, Dean J. Defective zonae pellucidae in Zp2-null mice disrupt folliculogenesis, fertility and development Defective zonae pellucidae in Zp2-null mice disrupt folliculogenesis, fertility and development. *Development* 2001;**128**:1119–1126.

Rosenfeldt MT, Valentino M, Labruzzo S, Scudder L, Favlaki M, Cao J, Vacirca J, Bahou WF, Zucker S. The organomercurial 4-aminophenylmercuric acetate (APMA), independent of matrix metalloproteinases (MMPs), induces dose-dependent activation/inhibition of platelet aggregation. *Thromb Haemost* 2005;**93**:326–330.

Sachdev M, Mandal A, Mulders S, Digilio LC, Panneerdoss S, Suryavathi V, Pires E, Klotz KL, Hermens L, Herrero MB *et al*. Oocyte specific oolemmal SAS1B involved in sperm binding through intra-acrosomal SLLP1 during fertilization. *Dev Biol* 2012;**363**:40–51.

Sato K. Polyspermy-preventing mechanisms in mouse eggs fertilized in vitro. *J Exp Zool* 1979;**210**:353–359.

Schmell ED, Gulyas BJ. Ovoperoxidase activity in ionophore treated mouse eggs. II. Evidence for the enzyme's role in hardening the zona pellucida. *Mol Reprod Dev* 1980;**3**:279–290.

Schneider CA, Rasband WS, Eliceiri KW. NIH Image to ImageJ: 25 years of image analysis. *Nat Methods* 2012;**9**:671–675.

Schroeder AC, Schultz RM, Kopf GS, Taylor FR, Becker RB, Eppig JJ. Fetuin inhibits zona pellucida hardening and conversion of ZP2 to ZP2f during spontaneous mouse oocyte maturation in vitro in the absence of serum. *Biol Reprod* 1990;**43**:891–897.

Smithberg M. The effect of different proteolytic enzymes on the zona pellucida of mouse ova. *Anat Rec* 1953;**117**:554.

Stork CJ, Li YV. Intracellular zinc elevation measured with a 'calcium-specific' indicator during ischemia and reperfusion in rat hippocampus: a question on calcium overload. *J Neurosci* 2006;**26**:10430–10437.

Stöcker W, Karmilin K, Hildebrand A, Westphal H, Yiallouros I, Weiskirchen R, Dietzel E, Floehr J, Jahnen-Dechent W. Mammalian gamete fusion depends on the inhibition of ovastacin by fetuin-B. *Biol Chem* 2014;**395**:1195–1199.

Szollosi D. Development of cortical granules and the cortical reaction in rat and hamster eggs. *Anat Rec* 1967;**159**:431–446.

Tawia SA, Lopata A. The fertilization and development of mouse oocytes following cortical granule discharge in the presence of a protease inhibitor. *Hum Reprod* 1992;**7**:1004–1009.

Wassarman PM, Jovine L, Litscher ES. Mouse zona pellucida genes and glycoproteins. *Cytogenet Genome Res* 2004;**105**:228–234.

Wessel GM, Brooks JM, Green E, Haley S, Voronina E, Wong J, Zaydfudim V, Conner S. The biology of cortical granules. *Int Rev Cytol* 2001;**209**:117–206.

Wolf DP, Hamada M. Induction of zonal and egg plasma membrane blocks to sperm penetration in mouse eggs with cortical granule exudate. *Biol Reprod* 1977;**17**:350–354.

Wolf DP, Soper K. Block to sperm penetration in zona-free mouse eggs. *Dev Biol* 1978;**64**:1–10.

Xiong B, Zhao Y, Beall S, Sadusky AB, Dean J. A unique egg cortical granule localization motif is required for ovastacin sequestration to prevent premature ZP2 cleavage and ensure female fertility in mice. *PLoS Genet* 2017;**13**:e1006580.

Yiallouros I, Kappelhoff R, Schilling O, Wegmann F, Helms MW, Auge A, Brachtendorf G, Berkhoff EG, Beermann B, Hinz HJ *et al*. Activation mechanism of pro-astacin: role of the pro-peptide, tryptic and autoproteolytic cleavage and importance of precise amino-terminal processing. *J Mol Biol* 2002;**324**:237–246.

Zhang X, Rutledge J, Khamsi F, Armstrong DT. Release of tissue-type plasminogen activator by activated rat eggs and its possible role in the zona reaction. *Mol Reprod Dev* 1992;**32**:28–32.